

Mechanisms of Large Actuation Strain in Dielectric Elastomers

Soo Jin Adrian Koh,^{1,2,3} Tiefeng Li,^{1,4} Jinxiong Zhou,^{1,5} Xuanhe Zhao,^{1,6}
Wei Hong,⁷ Jian Zhu,¹ Zhigang Suo¹

¹School of Engineering and Applied Sciences, Harvard University, Cambridge, Massachusetts 02138

²Institute of High Performance Computing, 1 Fusionopolis Way, #16-16 Connexis, Singapore 138632, Singapore

³Engineering Science Programme and Department of Civil and Environmental Engineering,
National University of Singapore, Kent Ridge, Singapore 119260, Singapore

⁴Institute of Applied Mechanics, Zhejiang University, 38 Zheda Road, Hangzhou, Zhejiang 310027, China

⁵MOE Key Laboratory of Strength and Vibration and School of Aerospace, Xi'an Jiaotong University, Xi'an 710049, China

⁶Soft Active Materials Laboratory, Department of Mechanical Engineering and Materials Science,
Duke University, Durham, North Carolina 27708

⁷Department of Aerospace Engineering, Iowa State University, Ames, Iowa 50011

Correspondence to: S. J. A. Koh (E-mail: kohsj@ihpc.a-star.edu.sg and ceeksja@nus.edu.sg)

Received 22 December 2010; revised 31 January 2011; accepted 31 January 2011; published online 2011

DOI: 10.1002/polb.22223

ABSTRACT: Subject to a voltage, a dielectric elastomer (DE) deforms. Voltage-induced strains of above 100% have been observed when DEs are prestretched, and for DEs of certain network structures. Understanding mechanisms of large actuation strains is an active area of research. We propose that the voltage-stretch response of DEs may be modified by prestretch, or by using polymers with “short” chains. This modification results in suppression or elimination of electromechanical instability, leading to large actuation strains. We propose a method to

select and design a DE, such that the actuation strain is maximized. The theoretical predictions agree well with existing experimental data. The theory may contribute to the development of DEs with exceptional performance. © 2011 Wiley Periodicals, Inc. *J Polym Sci Part B: Polym Phys* 49: 504–515, 2011

KEYWORDS: dielectric properties; elastomers; high performance polymers; strain; stimuli-sensitive polymers; theory; thermodynamics; tension

INTRODUCTION A dielectric elastomer (DE) transducer consists of a thin membrane of polymer, sandwiched between compliant electrodes. Subject to a voltage, the DE reduces in thickness and expands in area. This process is known as electrical actuation. Because of its fast response time, excellent conversion efficiency, and high specific energy, DEs have been proposed as artificial muscles, Braille displays, life-like robots, tunable lens, and power generators.^{1–7} When a DE is used as an actuator, it is desirable to achieve a large voltage-induced strain.^{8,9} This article presents a method to understand the mechanisms of large actuation strains, and a guide on how to use or select an elastomer, such that the actuation strain is maximized.

The maximum strain that can be induced by voltage is limited by multiple modes of DE failure.^{10–13} For instance, the DE may be over-stretched, leading to material rupture, or the voltage may be too high, leading to electrical breakdown (EB). Early experiments observe an actuation strain of about 3% in thermoplastic polyurethane films, under a high electric field of 20 MV/m.¹⁴ Pelrine et al. subsequently demonstrated that actuation strains of above 30% can be achieved using silicone DEs coated with compliant electrodes.¹⁵ This

work was followed with a prestretched polyacrylate very-high-bond (VHB) DE.^{8,16,17} Subject to an equal-biaxial pre-strain of 300%, area actuation strains of above 100% were observed.⁸ Recent experiments and analyses have shown that it is possible to introduce a second network to induce internal prestretch,^{9,18} thereby enhancing the actuation strain. Zhao and Suo recently proposed that, by selecting or designing an elastomer with suitable stress–strain response, giant actuation strains of above 500% is possible.¹⁹ Alternatively, it has also been demonstrated that, controlling the electric charge instead of voltage during actuation may also induce strains in excess of 100%.^{20,21}

While experimental studies have shown that the actuation strain of a DE actuator (DEA) may be enhanced by various methods like prestraining,⁸ designing elastomers with interpenetrating networks⁹ and swelling an elastomer with a solvent,²² the mechanism behind such enhancement remains to be further clarified. Some recent studies have attributed this enhancement to the increase in dielectric strength due to stretch,^{10,23,24} and strain-softening over the initial 200% stretch of a polyacrylate elastomer.²⁵ The accounts given in these studies attempts to explain specific DEA systems, but

may be limited in its generality. We therefore ask: What are the fundamental mechanisms behind large actuation strains in a DEA? For a given DEA, what is the theoretical limit for the actuation strain? How, therefore, does one maximize the actuation strain in the DEA?

Voltage-induced strain of a DE may be limited by electromechanical instability (EMI),²⁶ also known as pull-in instability. EMI is due to a positive feedback between an increasing electric field and a thinning DE, which may lead to EB. This instability may be suppressed or eliminated by prestretch, or by designing an elastomer with “short” polymer chains that restricts the limiting elastic strain to a sufficiently small value. The suppression or elimination of EMI leads to a significant enhancement in the actuation strain. We analyze the voltage-stretch response of a DE, under a constant, externally applied equal-biaxial prestress. We show that there is an optimal level of prestress that maximizes actuation strain. We produce phase diagrams that allow the user to select suitable elastomers of desired actuation response. Finally, we analyze a polyacrylate, VHB circular DEA, and show that our theory agrees very well with the experimental observations.⁸

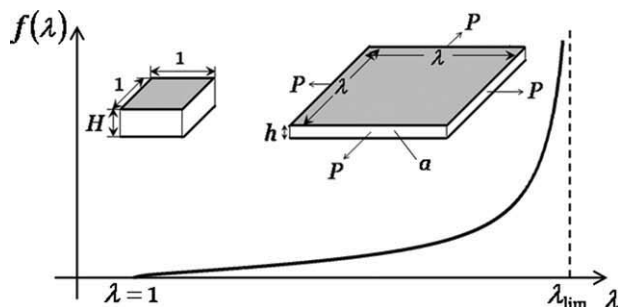
MECHANISMS OF LARGE ACTUATION STRAIN

An elastomer consists of a network of polymer chains, connected by covalent crosslinks. Polymer chains have varying degrees of flexibility. Polymer chains that are highly flexible can be highly coiled at their unstretched state, and will undergo very large deformation before they reach their fully stretched state. On the other hand, polymer chains that are less flexible will only undergo modest deformation before it becomes fully stretched. A network of fully stretched polymer chains makes the elastomer behave like a rigid bar; no deformation is possible under load. A typical elastomer exhibits nonlinear stress–strain behavior. The inset of Figure 1(a) illustrates the deformation of membrane of a DE subject to equal-biaxial forces P . In the unstressed state, the membrane is of unit area and thickness H . Subject to equal-biaxial forces P , the membrane is of planar area λ^2 and thickness h . The elastomer is taken to be incompressible, so that $H = h\lambda^2$. Write the stress-stretch curve as:

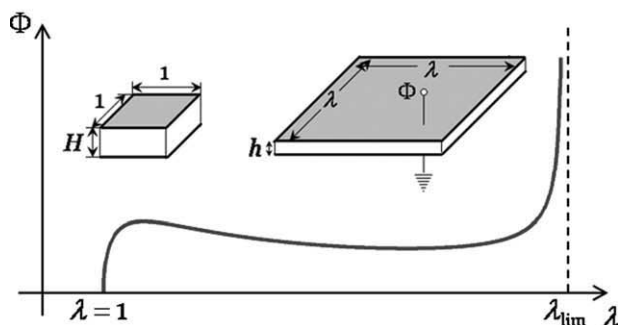
$$\sigma = f(\lambda) \quad (1)$$

where $\sigma = P/a$, and $a = h\lambda$ [inset Fig. 1(a)]. As illustrated in Figure 1(a), upon approaching the limiting stretch λ_{lim} , the elastomer stiffens steeply. That is, the maximum possible stretch of an elastomer is λ_{lim} , where the polymer chains attain their fully stretched states.

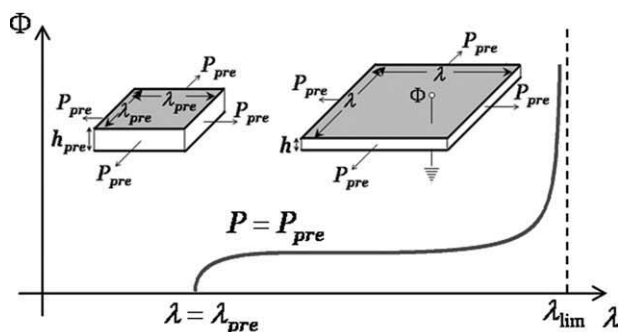
The same membrane can also deform under a voltage, in the absence of applied forces. Subject to a voltage Φ , charges of opposite signs on the two electrodes cause the membrane to expand in its area, and reduce in its thickness [Fig. 1(b)]. Every crosslinked polymer chain in the elastomer consists of a large number of monomers. Consequently, the crosslinks have negligible effect on the polarization of the monomers; the elastomer polarizes freely like a polymer melt. This theoretical observation is confirmed by experimental evidences



(a)



(b)



(c)

FIGURE 1 Deformation response of a dielectric elastomer (DE) subject to: (a) Equal-biaxial force only; (b) Voltage only; (c) Voltage with constant applied force (P_{pre}), λ_{pre} is the prestretch applied to the DE before voltage application. The voltage-stretch response of the DE [(b) and (c)] is modified by the application of prestretch. The salient point of this modification lies in the suppression or elimination of the peak in the voltage-stretch response, by prestretching.

in ref. 26, where the permittivity (ϵ) of an elastomer changes negligibly over a strain of 400%. We may therefore assume that the dielectric behavior of an elastomer is exactly the same as that of a polymer melt. Hence, the effect of the voltage on the deformation of the elastomer is equivalent to equal-biaxial Maxwell stress ϵE^2 ,^{15,27,28} where E is the electric field through the thickness of the membrane. In the

absence of an externally applied mechanical load, the equation of state is:

$$\varepsilon E^2 = f(\lambda) \quad (2)$$

Recall that $E = \Phi/h$ and $H = h\lambda^2$. We rewrite eq 2 as:

$$\Phi = \frac{H}{\sqrt{\varepsilon}} \lambda^{-2} \sqrt{f(\lambda)} \quad (3)$$

The voltage-stretch response of a DE may be readily interpreted from eq 3: For $f(\lambda)$ that takes the form shown in Figure 1(a), at small stretches, λ^{-2} decreases while $\sqrt{f(\lambda)}$ increases. As λ increases, the rate of decrease in λ^{-2} exceeds the rate of increase in $\sqrt{f(\lambda)}$; Φ hence attains a peak, and then drops [Fig. 1(b)]. However, as λ becomes very large, $\sqrt{f(\lambda)}$ recovers against λ^{-2} , and Φ increases again. In the limit of $\lambda \rightarrow \lambda_{\text{lim}}$, $\sqrt{f(\lambda)}$ dominates, leading to a near vertical Φ - λ trend. The physical interpretation of this voltage-stretch response is as follows: As voltage (Φ) is increased, the DE responds Φ to by an increase in stretch (λ). When Φ becomes sufficiently high, the same Φ induces an even higher electric field; a positive feedback develops between a thinning DE and an increasing electric field, indicating the onset of EMI.^{26,29} In a voltage-controlled actuation, at EMI, the deformation of the elastomer will “jump” from a small λ , to a very high λ . The elastomer may not survive this “jump” due to EB. As such, the maximum actuation strain may be severely limited by EMI. Hence, to increase the maximum actuation strain, it is desirable to minimize the magnitude of the “jump”, or to simply eliminate EMI. One way to do this is to move λ_{lim} closer to the peak (Fig. 2). In this case, $\sqrt{f(\lambda)}$ may dominate against λ^{-2} at small stretches, suppressing or eliminating the peak (Fig. 2).

Another way to suppress or eliminate EMI is to apply an external force P during the actuation of the DE [Fig. 1(c)]. The force gives rise to a mechanical stress $\sigma = P/\lambda h$. The mechanical stress and the Maxwell stress together cause the elastomer to deform, so that:

$$\sigma + \varepsilon E^2 = f(\lambda) \quad (4)$$

We rewrite this equation as:

$$\Phi = \frac{H}{\sqrt{\varepsilon}} \lambda^{-2} \sqrt{f(\lambda) - \frac{P\lambda}{H}} \quad (5)$$

The external force P may remain constant (P_{pre}), or vary during DE actuation. To illustrate essential ideas, we consider the case where a constant prestress is applied during DE actuation (P_{pre}). Applying P_{pre} has two effects on the Φ - λ curve. First, the prestress induces an initial strain on the elastomer, bringing the start point nearer to λ_{lim} [Fig. 1(c)]. This effect is similar to that of moving λ_{lim} closer to the peak of an unstressed DEA (Fig. 2). Second, comparing eqs 3 and 5, Φ required for actuation is reduced by the prestress. This reduction further suppresses the peak. The physical interpretation for the second effect is this: Prior to the appli-

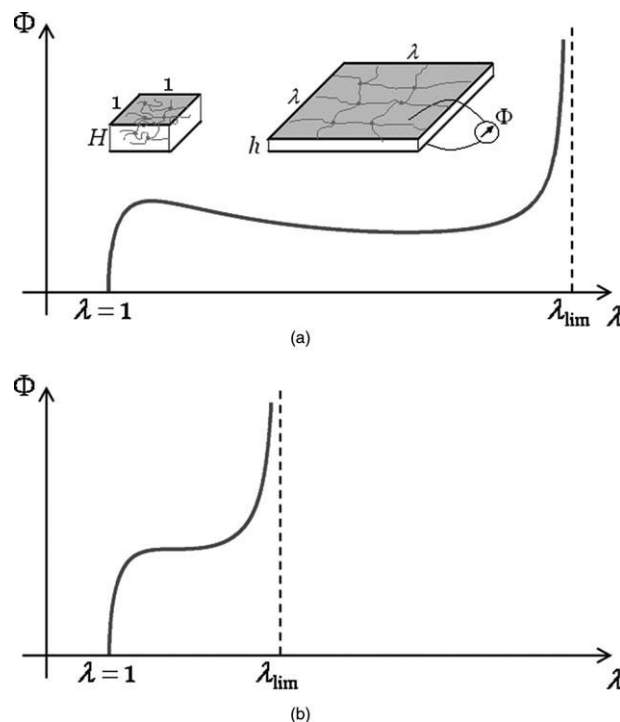


FIGURE 2 Electromechanical response dielectric elastomers (DE) with different degrees of polymer chain extensibility, in the absence of mechanical prestretch: (a) A very stretchable DE with large λ_{lim} , for instance, polyacrylate very-high-bond (VHB) DE; (b) A less stretchable elastomer with smaller λ_{lim} , for instance silicone DE or elastomers with interpenetrating networks. λ_{lim} is determined by the chain extensibility. For a sufficiently small λ_{lim} , the voltage-stretch response is modified, such that the peak is eliminated. This effect resembles that of a prestretched DE.

cation of a voltage, a prestressed elastomer is thinner than an unstressed elastomer. Hence, the voltage Φ required to induce the same electric field in a prestressed elastomer is smaller than that of an unstressed elastomer. These two effects of prestress combine to produce an effective suppression and elimination of the peak.

Examining Figures 1(b,c) and 2(a,b), two distinct types of voltage-stretch response may be identified: One type exhibits EMI, as indicated by a peak in the Φ - λ curve [Figs. 1(b) and 2(a)]. We call this the Type A response. The other does not exhibit any EMI; the stretch increases monotonically with voltage [Figs. 1(c) and 2(b)]. We call this the Type B response. An elastomer may switch from a Type A response to a Type B response by prestretch and/or by selecting an elastomer with a smaller λ_{lim} .

We next ask the question: What is the maximum actuation strain for a DEA? To answer this, we have to consider the modes that lead to irrecoverable failure of the DEA during actuation. Two of which are EB, and failure by rupture. The former occurs when the electric field exceeds the EB limit of the elastomer. This limit is determined by its dielectric strength (E_B). The latter occurs when the elastomer is

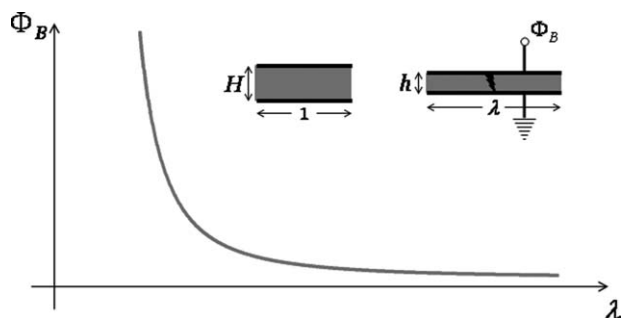


FIGURE 3 A dielectric elastomer (DE) may fail by electrical breakdown. The voltage that causes breakdown is Φ_B . The corresponding electric field at breakdown is $E_B = \Phi_B/h$, which is also known as the dielectric strength. Assuming that E_B is known, the equation that describes the above relationship is: $\Phi_B = E_B H \lambda^{-2}$, where λ is the stretch at breakdown.

overstretched. Overstretching causes existing cracks in the polymer matrix to propagate, which will inadvertently lead to the tearing of the elastomer.^{9,29} In this analysis, we have assumed that great care has been taken to manufacture the elastomer, so that EB always precedes rupture. For a DE under equal-biaxial loading, the voltage that corresponds to EB (Φ_B) is:

$$\Phi_B = E_B H \lambda^{-2} \quad (6)$$

This relationship is plotted in Figure 3. Experiments have suggested that E_B may be modified by stretch.^{10,30} This observation may be easily incorporated into eq 6 by using a power-law relationship: $E_B = E_B(1)\lambda^R$, where $E_B(1)$ is the dielectric strength when the stretch is held at $\lambda = 1$, and R measures the degree of sensitivity of E_B towards stretch.²⁹ The effect of increase in dielectric strength due to stretch, leading to an enhancement in actuation, has been discussed in other studies,^{10,23,24,31} and shall not be repeated here. We will assume a fixed E_B in our analyses.

Figure 4 shows three possible routes to EB failure for a Type A DE. Under a monotonically increasing voltage, Figure 4(a) represents a DE of “stiff” electromechanical response. Such DEs have very low dielectric strength and dielectric constant, and high mechanical stiffness. The DE does not deform much by electrical actuation, resembling that of a piezoceramic actuator.³² The maximum actuation strain ($\lambda_{fail}/\lambda_{pre} - 1$) is typically less than 10%.^{14,32} We classify it as a Type A_I. Figure 4(b) shows a highly deformable DE that undergoes EMI, leading to EB. This DE could not survive the “jump”, also known as the “snap-through” deformation.²⁸ Such DEs have moderate to high dielectric strength and dielectric constant, and low mechanical stiffness. Maximum actuation strain ($\lambda_{fail}/\lambda_{pre} - 1$) for such elastomers is less than 30%.¹⁵ We classify this as a Type A_{II}. Figure 4(c) represents a DE that undergoes EMI, and survives the “snap-through” deformation. Such DEs have exceptionally high dielectric strength and dielectric constant, and low mechanical stiffness. Maximum actuation strain ($\lambda_{fail}/\lambda_{pre} - 1$) may exceed 1000%.¹⁸ We classify this as a Type A_{III}. However,

DEs with such actuation performance have not been discovered. Nevertheless, we note that a suitably modified voltage-stretch response may suppress the peak, thereby allowing the DE to survive the “snap-through” deformation.

The Type B voltage-stretch response allows the actuation strain to increase monotonically with the voltage (Fig. 5). As such, the DE does not undergo EMI. The maximum actuation strain ($\lambda_{fail}/\lambda_{pre} - 1$) is determined by EB. As a result, large

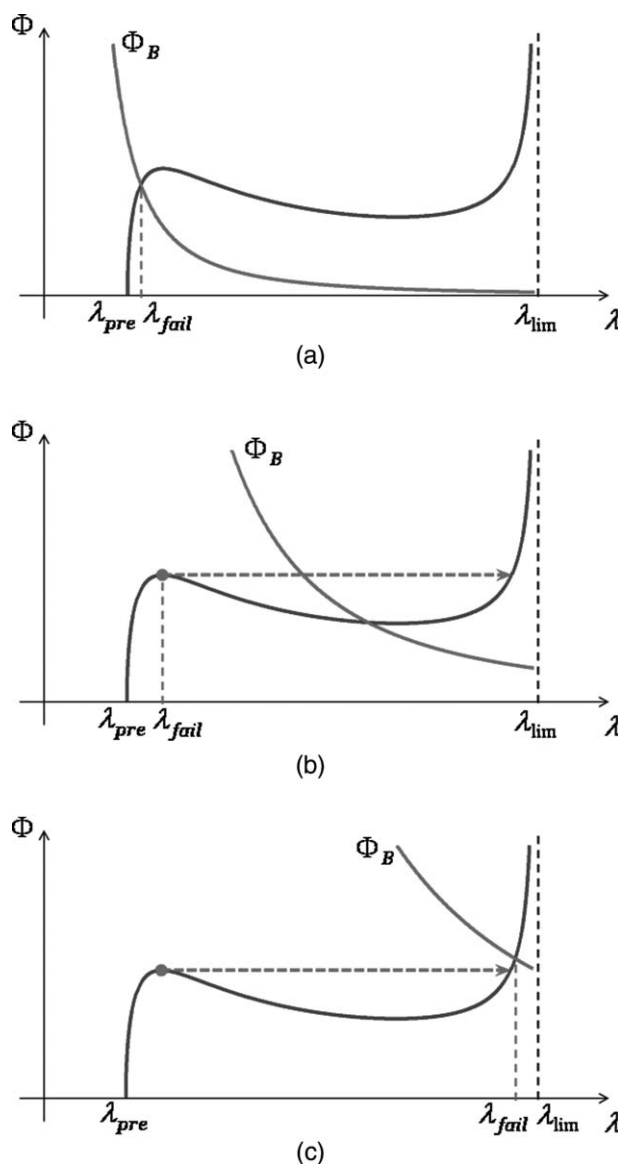


FIGURE 4 Under a monotonically increasing voltage, a Type A dielectric elastomer actuator (DEA) may fail by: (a) Electrical breakdown with small actuation strain (Type A_I); (b) Electromechanical instability leading to electrical breakdown, it fails at the point where instability occurs. The DEA does not survive the “snap-through” deformation (Type A_{II}); (c) Electrical breakdown with giant actuation strain, the DEA survives the “snap-through” deformation (Type A_{III}). The route to failure is determined by the location of the breakdown line.

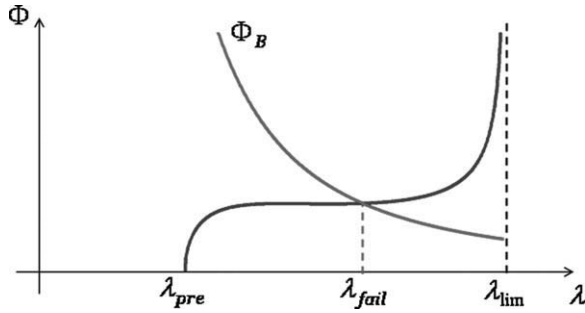


FIGURE 5 Under a monotonically increasing voltage, a Type B dielectric elastomer actuator (DEA) fails only by electrical breakdown.

strains of actuation may be realized. Strains of actuation of above 100% have been observed in prestretched polyacrylate DEs.⁸ Similar enhancements have also been observed in DEs with interpenetrating networks,⁹ where the limiting stretch (λ_{lim}) of an elastomer is reduced by introducing an additional polymer network on top of an existing stretched network (see this effect in Fig. 2).

In this section, we have identified mechanisms of large actuation strain: The suppression or elimination of EMI, by modifying the voltage-stretch response. This modification could be achieved by prestretch and/or by selecting an elastomer with sufficiently small limiting stretch. We have classified the voltage-stretch response of DEAs into Type A and Type B. We have further classified the routes to failure into Types A_I, A_{II}, A_{III} and B, which determines the maximum actuation strain of the DEA. Zhao and Suo¹⁹ have previously adopted a similar method of classification. In their method, A_I is classified as Type I [Fig. 4(a)], A_{II} is classified as Type II [Fig. 4(b)], and A_{III} and B are jointly classified as Type III [Figs. 4(c) and 5]. They have made no effort to differentiate between a DEA that could survive a “snap through” deformation (A_{III}) and a DEA with a monotonic voltage-stretch response (B). This differentiation is important in identifying DEAs that are capable of giant actuation strain. We shall show in “Actuation of a DE Membrane under a Constant, Equal-Biaxial Prestress” section that a Type A_{III} is capable of producing a very high actuation strain, whereas Type B may not. In the following section, we will present the equations of state for a DE under general loading conditions, followed by an analysis of a DE membrane under constant, equal-biaxial prestress. Finally, a circular DEA⁸ will be analyzed. Using realistic experimental data, we verify that our model has good agreement with experimental observations.

EQUATIONS OF STATE FOR DEs

Subject to externally applied mechanical stresses σ_1 and σ_2 and electric field E , the equations of state for a DE are^{33–36}:

$$\sigma_1 + \varepsilon E^2 = \lambda_1 \frac{\partial W(\lambda_1, \lambda_2)}{\partial \lambda_1} \tag{7a}$$

$$\sigma_2 + \varepsilon E^2 = \lambda_2 \frac{\partial W(\lambda_1, \lambda_2)}{\partial \lambda_2} \tag{7b}$$

where $W(\lambda_1, \lambda_2)$ is the elastic free energy density function of the elastomer. λ_1 and λ_2 are the inplane stretches, and ε is the dielectric permittivity of the elastomer. Assuming incompressibility: $\lambda_3 = \lambda_1^{-1}\lambda_2^{-1}$. We have further assumed an ideal DE, whereby the dielectric permittivity is not significantly affected by stretch, exhibiting a liquid-like dielectric response.^{28,37} For a DE of unit planar dimensions, with thickness H at the undeformed state [Fig. 6(a)], σ_1 and σ_2 are related to the applied loads P_1 and P_2 as: $\sigma_1 = \lambda_1 P_1 / H$ and $\sigma_2 = \lambda_2 P_2 / H$. The electric field E is related to the applied voltage as: $E = \Phi / h$. Assuming incompressibility: $h = \lambda_1^{-1}\lambda_2^{-1}H$. Subject to P_1 and P_2 and voltage Φ through its thickness, the DE deforms to the actuated state [Fig. 6(b)].

For a hyperelastic material, the right-hand side of eq 7 gives the stress-strain relationship of the elastomer. One particular form for the free energy density function is^{38,39}:

$$W(\lambda_1, \lambda_2) = NkTn \left(\frac{\zeta}{\tanh \zeta} - 1 + \log \frac{\zeta}{\sinh \zeta} \right) \tag{8}$$

where kT is the temperature in the unit of energy, ζ is the normalized force in each chain, and N is the number of chains per unit volume, which is also proportional to the number of chemical crosslinks per unit volume. The stretch on each polymer chain Λ is related to the normalized force ζ as:

$$\Lambda = \sqrt{n} \left(\frac{1}{\tanh \zeta} - \frac{1}{\zeta} \right) \tag{9}$$

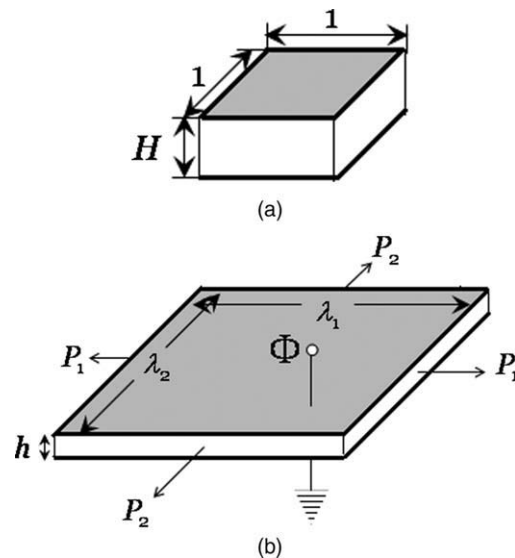


FIGURE 6 A dielectric elastomer actuator subject to general loading conditions P_1, P_2 and Φ : (a) At the undeformed state; (b) At the actuated state.

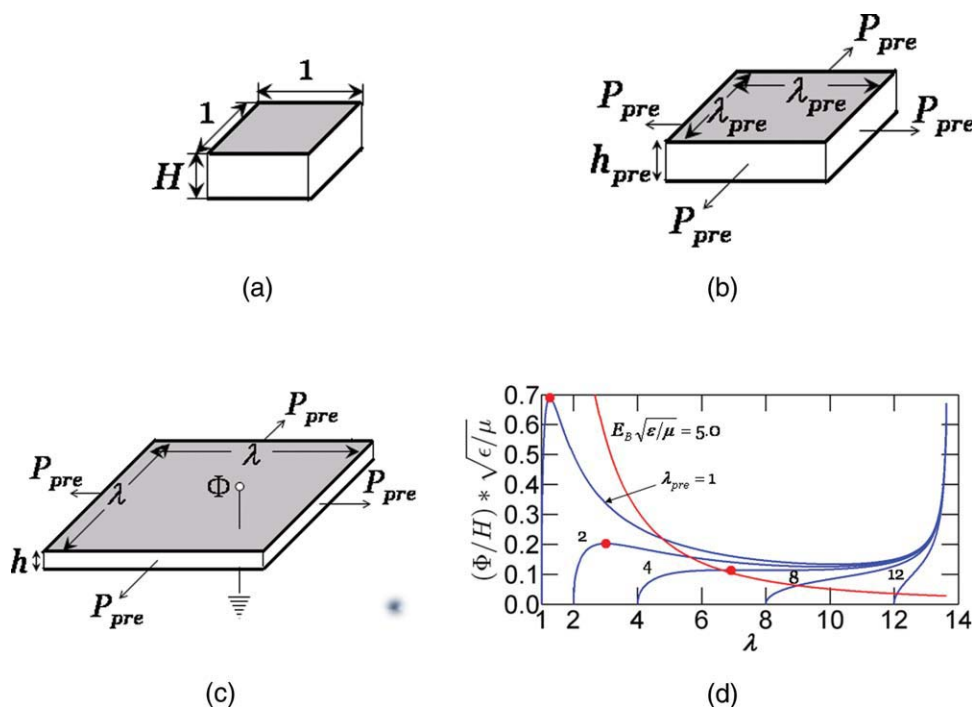


FIGURE 7 Analysis of a dielectric elastomer (DE) membrane subject to a constant, equal-biaxial prestress (a) DE membrane at the undeformed state; (b) DE membrane at the prestretched state; (c) DE membrane subject to voltage, with prestress maintained at P_{pre} ; (d) Voltage-stretch response of DE membrane at various prestretches λ_{pre} (blue lines), with electromechanical instability denoted with solid red dots, and electrical breakdown denoted by the intersection between the blue and the red lines.

where n is the number of statistical links in the chain, which determines the flexibility and limit stretch (λ_{lim}) of the chain. For an elastomer subject to principal stretches λ_1 and λ_2 , Arruda and Boyce³⁹ proposed that:

$$\Lambda = \sqrt{\frac{\lambda_1^2 + \lambda_2^2 + \lambda_1^{-2}\lambda_2^{-2}}{3}} \quad (10)$$

In the limit where $n \rightarrow \infty$ and $\zeta \rightarrow 0$, the polymer chains exhibit infinite flexibility ($\lambda_{lim} \rightarrow \infty$), and the Neo-Hookean model is recovered. The small strain shear modulus is given as: $\mu = NkT$. When $\Lambda \rightarrow \sqrt{n}$, the stretches approach their limits according to eq 10. Differentiating eq 8, combining eqs 9 and 10, and substituting into eq 7, we have:

$$\sigma_1 + \varepsilon E^2 = \mu \zeta \sqrt{n} \frac{\lambda_1^2 - \lambda_1^{-2}\lambda_2^{-2}}{3\Lambda} \quad (11a)$$

$$\sigma_2 + \varepsilon E^2 = \mu \zeta \sqrt{n} \frac{\lambda_2^2 - \lambda_1^{-2}\lambda_2^{-2}}{3\Lambda} \quad (11b)$$

Equation 11 suggests that the stress-strain relationship is governed by two material parameters μ and n . The former determines the slope of the stress-strain curve at small strains, and the latter determines the limiting stretch (λ_{lim}) of the elastomer. Given a loading program σ_1 , σ_2 and E (and hence, P_1 , P_2 , and Φ), the deformation of the DE can be solved from eqs 7-11.

The generality of eq 7 allows the user to select more elaborate $W(\lambda_1, \lambda_2)$ that may include more material parameters.^{40,41} For instance, a model that captures the physical entanglements between highly coiled polymer chains⁴¹ gives rise to a more rapid rate of softening in the initial 200% strain, when compared with the form used in eq 8. This model may be very informative for the determination of a more exact response before the onset of EMI but will not change our qualitative conclusions pertaining to actuation enhancement due to prestretch.

ACTUATION OF A DE MEMBRANE UNDER A CONSTANT, EQUAL-BIAXIAL PRESTRESS

The deformation response of a DE depends on the loading configuration. To illustrate essential ideas, we consider a DE membrane subject to equal-biaxial tension [Fig. 7(a-c)]. At the undeformed state [Fig. 7(a)], the DE has unit dimensions and thickness H . An equal-biaxial prestretch is applied in the absence of voltage, to state Figure 7(b). Maintaining a constant prestress (P_{pre}), a voltage is applied to the DE, resulting in further deformation up to the actuated state Figure 7(c). Substituting $\lambda_1 = \lambda_2 = \lambda$, $\sigma_1 = \sigma_2 = \sigma = (P/H)\lambda$ and $E = (\Phi/H)\lambda^4$ into eqs 7-11, combining and simplifying, we have:

$$\frac{P}{\mu H} + \frac{\varepsilon}{\mu} \left(\frac{\Phi}{H}\right)^2 \lambda^3 = \zeta \sqrt{n} \frac{\lambda - \lambda^{-5}}{3\Lambda} \quad (12)$$

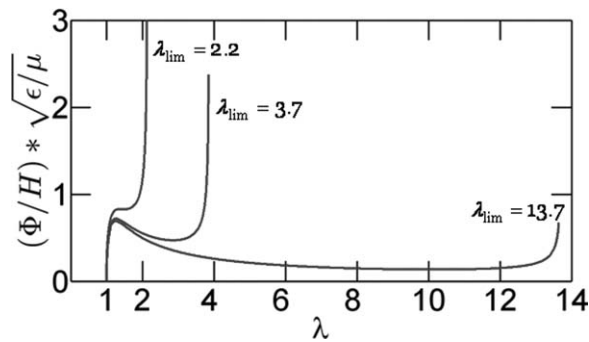


FIGURE 8 A dielectric elastomer membrane with “short” polymer chains (small λ_{lim}) does not experience electromechanical instability under electrical actuation. This may be achieved by designing an elastomer with interpenetrating networks, pre-swelling an elastomer or an elastomer with significant amounts of side chains. When $\lambda_{\text{lim}} = 2.2$ the voltage-stretch response switches from Type A to Type B.

The left-hand side of eq 12 denotes the loading program (P and Φ), and the right-hand side is the nondimensionalized stress-strain relationship. Putting $\Lambda = \sqrt{n}$ in eq 10, the limiting stretch (λ_{lim}) is related to n as:

$$n = \frac{2\lambda_{\text{lim}}^2 + \lambda_{\text{lim}}^{-4}}{3} \quad (13)$$

At the prestretched state, λ_{pre} is chosen, and P_{pre} is computed from eq 12 by setting $\Phi = 0$. Keeping a constant prestress $P = P_{\text{pre}}$, the voltage-stretch response of the prestressed elastomer is plotted. From eq 12, when $\lambda_{\text{pre}} = 1.0$, $P_{\text{pre}} = 0.0$. This corresponds to an unstressed DE under voltage-induced actuation. We consider an elastomer with highly stretchable polymer chains, with $\lambda_{\text{lim}} = 13.7$. From eq 12, we have $n = 125$, which represents elastomers such as polyacrylate VHB dielectrics.³⁸ Figure 7(d) plots the voltage-stretch response of the DE at various levels of prestretch λ_{pre} . This plot uses a nondimensionalized quantity for the voltage: $(\Phi/H)\sqrt{\epsilon/\mu}$, and a corresponding nondimensionalized quantity for the EB field: $E_B\sqrt{\epsilon/\mu}$.

From Figure 7(d), we observe that EMI is significantly suppressed at $\lambda_{\text{pre}} = 4.0$. For $\lambda_{\text{pre}} < 4.0$, the membrane follows a Type A_{II} response [Fig. 4(b)]. An examination of Figure 7(d) gives an actuation strain of about 26% when $\lambda_{\text{pre}} = 1.0$. When prestretched to $\lambda_{\text{pre}} = 4.0$, the actuation strain increases to 73%, which corresponds to an area actuation strain of about 200%. The source of this increase in actuation strain is the suppression of EMI by prestretch.

Let us consider the other way to suppress EMI—we select an elastomer with lower limiting stretches (λ_{lim}). Figure 8 illustrates this by considering three elastomers of different λ_{lim} : 13.7, 3.7, and 2.2. An elastomer with $\lambda_{\text{lim}} = 3.7$ suppresses EMI. An elastomer with $\lambda_{\text{lim}} = 2.2$ eliminates EMI. Examples of such classes of elastomers include silicone elastomers,⁴² elastomers with interpenetrating networks,⁹ and preswelled elastomers.²²

We shall now summarize these observations in the form of phase diagrams that define regions of A_I, A_{II}, A_{III}, and B (Fig. 9). In these phase diagrams, for a given $E_B\sqrt{\epsilon/\mu}$, we represent these regions on a $\lambda_{\text{lim}} - \lambda_{\text{pre}}$ plane. Figure 9 may be interpreted as follows: for a point on the plane, a unique voltage-stretch response is defined. The response follows a Type A (Fig. 4), if λ_{lim} is high and λ_{pre} is low. It follows a Type B response (Fig. 5) if λ_{lim} is low and λ_{pre} is high. For a Type A with a low $E_B\sqrt{\epsilon/\mu}$ [Fig. 9(a)], it fails predominantly by Type A_I, representing a “stiff dielectric” [Fig. 4(a)]. For higher values of $E_B\sqrt{\epsilon/\mu}$ [Figs. 9(b–d)], Type A_{II} is the predominant route to failure; the DEA fails after the onset of EMI and does not survive the “snap-through” deformation [Fig. 4(b)]. For a limited combination of λ_{pre} , λ_{lim} , and $E_B\sqrt{\epsilon/\mu}$, the DEA survives the “snap-through” deformation, giving Type A_{III} [Fig. 4(c)] and may attain giant actuation strain. Figure 9 may be used as follows: for a given elastomer with known material properties (λ_{lim} and $E_B\sqrt{\epsilon/\mu}$), a horizontal line on the diagram characterizes the response of the elastomer at various levels of prestretch (λ_{pre}). Alternatively, one may be constrained to operate a DEA at a fixed level of λ_{pre} . In this case, a vertical line may be drawn on the diagram. This line may aid the selection of an elastomer with a suitable λ_{lim} that gives the desired voltage-stretch response. These diagrams may further be used to predict the maximum actuation strain of a given elastomer. We shall illustrate the method for an elastomer with $\lambda_{\text{lim}} = 13.7$, represented by the horizontal dashed lines in Figure 9.

The horizontal dashed lines on Figure 9 cut across various routes that the DEA may fail (A_I, A_{II}, A_{III}, and B). The maximum actuation stretch ($\lambda_{\text{fail}}/\lambda_{\text{pre}}$) is computed in accordance with Figure 4(a) (A_I), Figure 4(b) (A_{II}), Figure 4(c) (A_{III}), or Figure 5 (B). Figure 10 shows $\lambda_{\text{fail}}/\lambda_{\text{pre}}$ for an elastomer given by the horizontal lines in Figure 9. For the lowest $E_B\sqrt{\epsilon/\mu} = 1.0$, the DEA fails either by A_I or B; EMI does not occur. If $E_B\sqrt{\epsilon/\mu}$ is increased by an order of magnitude to 10.0, the DEA survives a “snap-through” deformation when $\lambda_{\text{pre}} = 4.0$, resulting in a very large actuation stretch of $\lambda_{\text{fail}}/\lambda_{\text{pre}} = 2.35$. For intermediate levels of $E_B\sqrt{\epsilon/\mu}$, a significant increase in the actuation stretch was observed when EMI is suppressed by increasing prestretch, attaining a maximum when EMI is averted (A_{II} → A_I, A_{III} or B). Figure 10 also shows that it is not necessarily true that large actuation strains may be attained for a Type B (monotonic voltage-stretch). This method may be used to determine the optimal prestretch that maximizes the actuation strain. The same procedure may be repeated if λ_{pre} is fixed. A vertical line drawn at the level of fixed λ_{pre} will allow an elastomer with the desired λ_{lim} to be selected. This method may further be used to analyze DEAs with other load configurations,^{8,10,13,42,43} nonideal electrostrictive DEs (dielectric constant is modified by stretch⁴⁴), and DEs with dielectric strengths that vary with stretch.^{10,37} In the following section, we shall illustrate our method on a particular configuration of DEA—the circular DEA, which is made of polyacrylate VHB elastomer. Our analysis is compared with existing experimental data.⁸

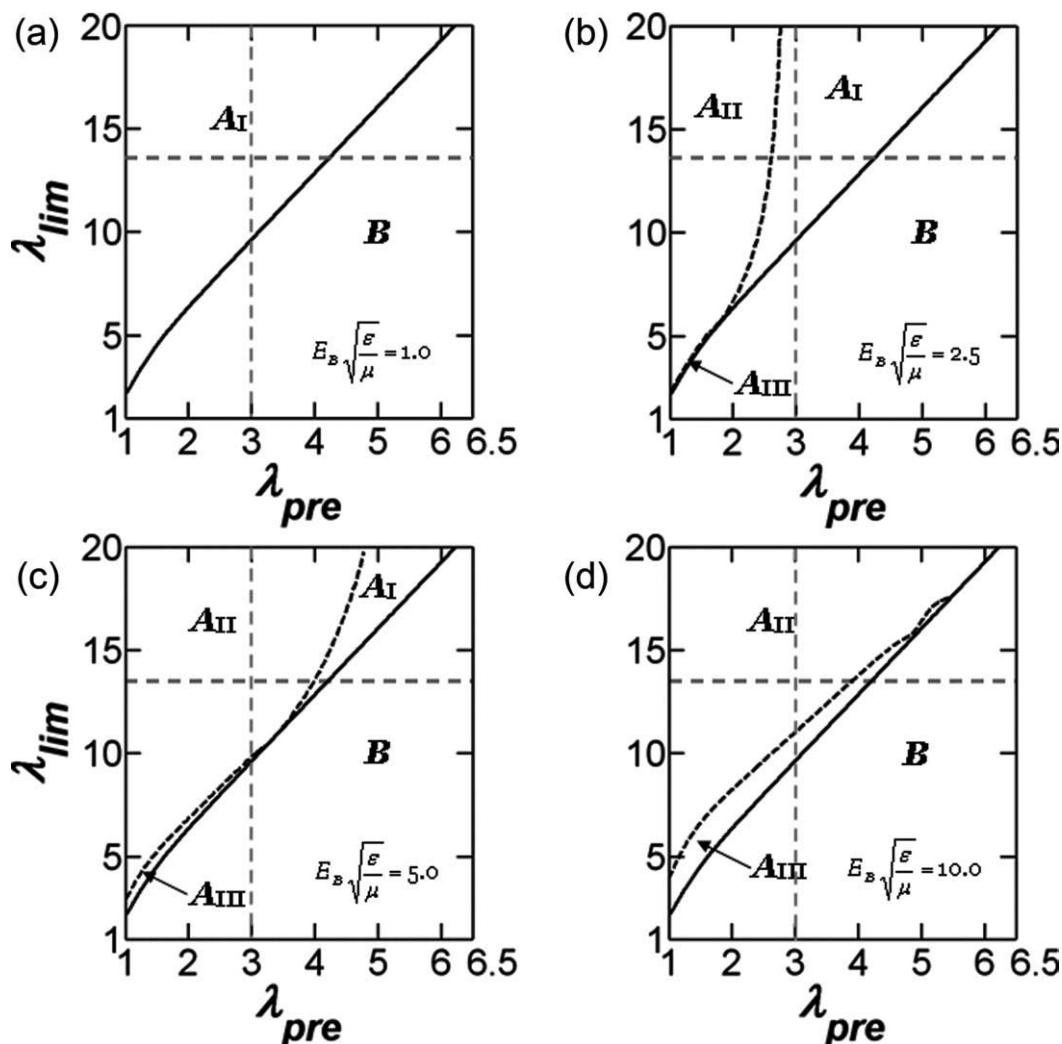


FIGURE 9 Phase diagrams for voltage-stretch response and route to failure of dielectric elastomer membrane actuators (A_I, A_{II}, A_{III}, and B) under constant, equal-biaxial prestress for: (a) $E_B \sqrt{\epsilon/\mu} = 1.0$; (b) $E_B \sqrt{\epsilon/\mu} = 2.5$; (c) $E_B \sqrt{\epsilon/\mu} = 5.0$; (d) $E_B \sqrt{\epsilon/\mu} = 10.0$. Horizontal lines maps the various routes to failure a specific elastomer across varying levels of prestretches (λ_{pre}). Vertical line maps the various routes to failure for various elastomers (of varying λ_{lim}) where λ_{pre} is fixed.

ACTUATION OF A CIRCULAR DEA

A DE membrane of circular actuator configuration is analyzed (Fig. 11). This particular configuration is commonly used to evaluate the voltage-induced actuation performance of a DE.^{8,35,43} This configuration consists of an active electrode area (region A), and a passive area with no electrodes (region B). At the undeformed state [Fig. 11(a)], the radius of region A is A , and the radius of region B is B . For an arbitrary point in region B, its radial distance from the center of the actuator is R . The membrane is first prestretched (λ_{pre}), and glued to a rigid frame [Fig. 11(b)]. After a long time, the deformation equilibrates with the applied stress; the stretched area of region A is computed, given as: $\pi A^2 \lambda_{pre}^2$. A voltage is then applied on region A. A further time is allowed to elapse, to allow the expanding region A to attain a new state of equilibrium [Fig. 11(c)]. The area is: $\pi A^2 \lambda_A^2$. This pro-

cess is repeated with increasing voltage, until failure occurs. The final area in region A is then computed, given as: $\pi A^2 \lambda_{fail}^2$. The area actuation stretch is computed as: $\lambda_{fail}^2 / \lambda_{pre}^2$. As region A is in a state of equal-biaxial deformation, the linear actuation stretch is $\lambda_{fail} / \lambda_{pre}$.

During the process of actuation, the active region A expands against the passive region B. In the case of a membrane with no prestretch ($\lambda_{pre} = 1$), a small voltage will induce a compressive stress on region A. A thin membrane cannot sustain any compressive stresses and will experience an out-of-plane buckling. This is manifested as wrinkles in the active region A (for instance, see Fig. 14 in ref. 10). This condition is termed the loss of tension (LT). Our analysis will terminate at the point of LT, as analysis beyond this point will require the consideration of complicated wrinkled geometry, which will not be the focus of this article.

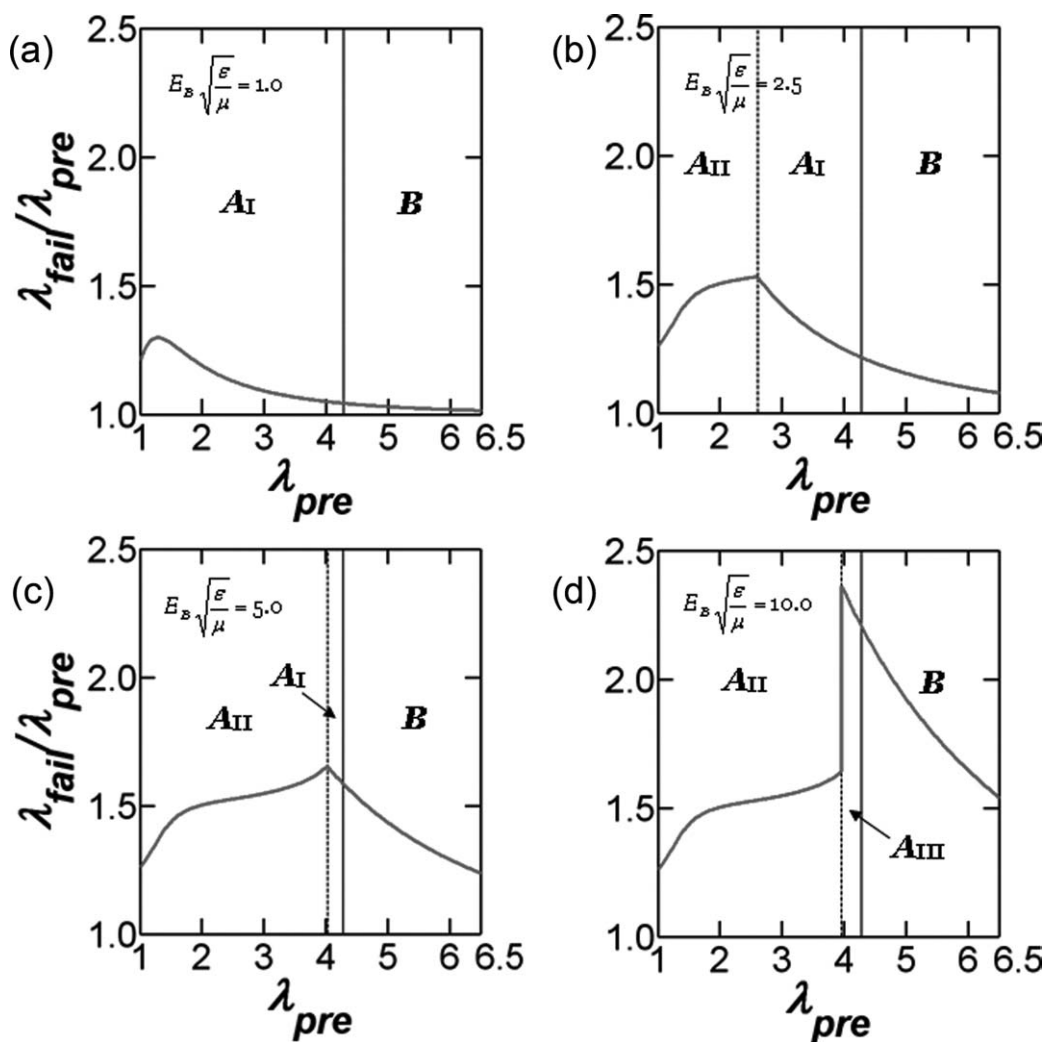


FIGURE 10 Actuation strains at failure for a dielectric elastomer membrane with $\lambda_{lim} = 13.7$, and (a) $E_B\sqrt{\epsilon/\mu} = 1.0$; (b) $E_B\sqrt{\epsilon/\mu} = 2.5$; (c) $E_B\sqrt{\epsilon/\mu} = 5.0$; (d) $E_B\sqrt{\epsilon/\mu} = 10.0$, plotted as functions of the equal-biaxial prestretch λ_{pre} . Regions of various routes to failure (A_I , A_{II} , A_{III} , and B) are denoted on the plot.

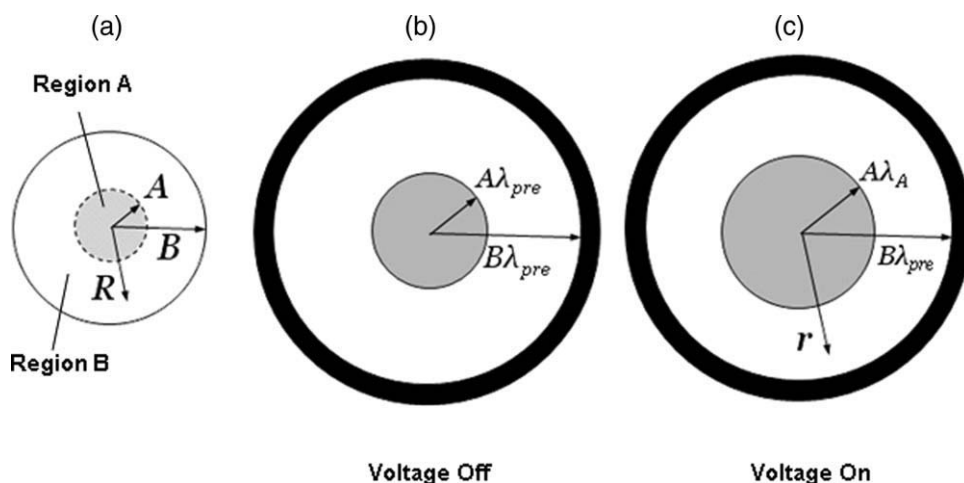


FIGURE 11 Schematic of the circular dielectric elastomer: (a) At undeformed state; (b) At prestretched state, with no voltage; (c) At actuated state, voltage is turned on, and region A expands.

As mentioned above, the active region A undergoes homogeneous, equal-biaxial deformation. The passive region B undergoes inhomogeneous, unequal-biaxial deformation. By geometry, the radial stretch (λ_R) for region B is given as:

$$\lambda_R = \frac{dr(R)}{dR} \quad (14a)$$

And the hoop stretch (λ_θ) is given as:

$$\lambda_\theta = \frac{r(R)}{R} \quad (14b)$$

where R is the radial distance of a particle from the center of the actuator at the undeformed state, and r is the radial distance of the same particle at the actuated state [Fig. 11(c)], and r is a function of R . Equilibrium gives:

$$\frac{ds_R(R)}{\partial R} + \frac{s_R(R) - s_\theta(R)}{R} = 0 \quad (15)$$

where s_R and s_θ are the nominal stresses in the radial and the hoop directions, related to the true stresses as: $s_R = \sigma_R/\lambda_R$ and $s_\theta = \sigma_\theta/\lambda_\theta$. From eqs 8–11, setting $\varepsilon E^2 = 0$, and because the principal directions “1” and “2” are equivalent to the radial and hoop directions R and θ , we have:

$$\frac{\partial \lambda_R}{\partial R} = \frac{1}{R} \left[\frac{\partial^2 W(\lambda_R, \lambda_\theta)}{\partial \lambda_R^2} \right]^{-1} \left[\frac{\partial W(\lambda_R, \lambda_\theta)}{\partial \lambda_\theta} - \frac{\partial W(\lambda_R, \lambda_\theta)}{\partial \lambda_R} \right] \quad (16a)$$

Combining eq 14, we have:

$$\frac{\partial \lambda_R}{\partial R} = \frac{1}{R} (\lambda_\theta - \lambda_R) \quad (16b)$$

Equation 16 gives a set of ordinary differential equations (ODEs), defining a boundary value problem for inhomogeneous deformation in region B. The inner boundary for this problem is at the interface between regions A and B ($R = A$), and the outer boundary is at the rigid frame ($R = B$). Considering force balance in the radial direction at $R = A$:

$$s_A = s_R \quad (17)$$

As region A is under homogeneous, equal-biaxial deformation, and observing that region A is subject to a voltage Φ , putting $\sigma_1 = \sigma_2 = \sigma_A$, $\lambda_1 = \lambda_2 = \lambda_A$ into eq 11, knowing that $s_A = \sigma_A/\lambda_A$ and $E = (\Phi/H)\lambda_A^{-2}$, we have:

$$s_A = \mu \zeta \sqrt{n} \frac{\lambda_A - \lambda_A^{-5}}{3\Lambda} - \varepsilon \left(\frac{\Phi}{H} \right)^2 \lambda_A^3 \quad (18)$$

Applying no-slip displacement boundary condition at $R = A$ gives:

$$\lambda_A = \lambda_\theta \quad (19)$$

Finally, applying no-slip displacement boundary condition at $R = B$ gives:

$$\lambda_\theta(R = B) = \lambda_{pre} \quad (20)$$

To obtain the voltage-stretch response in region A, we need to consider the interaction between the active region A and the passive region B. This is done by solving the ODEs in eq 16, using the boundary conditions eq 17–20, as follows: λ_A is first prescribed. From eq 19, we obtain the hoop stretch in region B, at $R = A$. The shooting method is then used to solve the ODEs given in eq 16. This was done by providing an initial guess to the radial stretch for region B (λ_R) at $R = A$. Equation 16 is then solved using eqs 8–11 and eqs 17 and 18, to obtain the stretches at $R = B$. If eq 20 is not satisfied, the radial stretch is iterated by the Newton-Raphson method, until eq 20 is satisfied within a prescribed error of deviation. Once λ_R at $R = A$ is known, s_A can be computed, and the voltage Φ required to cause λ_A can be obtained from eq 18.

The voltage-stretch response of region A could depend on the undeformed ratio of radii between regions A and B. The quantity B/A was not explicitly specified in the study.⁸ Hence, we used commonly adopted values of: $B/A = 2, 5, 10$, and 20.^{35,43} We further use the experimentally measured dielectric strength of polyacrylate VHB elastomers at prestretches of $\lambda_{pre} = 1.15$, and $\lambda_{pre} = 4.0$. They are given in ref. 8 as $E_B = 55\text{MV/m}$ and $E_B = 412\text{MV/m}$, respectively. Other material properties for VHB are given in refs. 27 and 36 as: $\lambda_{lim} = 13.7$, $\mu = 0.068\text{MPa}$ and $\varepsilon = 4.5\varepsilon_0$. Figure 12 shows the voltage-stretch behavior for circular DEAs over different B/A , at various levels of prestretch between $\lambda_{pre} = 1.15$ and $\lambda_{pre} = 12.0$. Two solid (red) EB lines are also drawn, which represent the two E_B values, measured for VHB at prestretches of $\lambda_{pre} = 1.15$ and $\lambda_{pre} = 4.0$.

Figure 12 shows that for $B/A < 10$, the voltage-stretch response and hence, the maximum actuation strain, is sensitive to B/A . This is due to the proximity of the rigid frame to the active region A, which imposes a significant constraint on the voltage-induced expansion of region A, through the passive region B. At $B/A = 2$, for $\lambda_{pre} \leq 4.0$, region A experiences LT (where internal stresses in region A become compressive, denoted by a cross \times) before it undergoes EB (denoted by the intersection between the blue voltage-stretch lines, and the red EB lines) or EMI (denoted by a solid red circle). For $B/A \geq 5$, EB or EMI generally precedes LT, as the constraint imposed by the rigid frame, through the much larger passive region B on A, is reduced. The maximum actuation stretch is computed based on the occurrence of EB, EMI, or LT, whichever comes first. However, experimentally, it has been shown that a DEA may undergo significant actuation after LT,¹⁷ but the amount of actuation stretch after LT depends on the geometrical and loading configuration, and shall not be further discussed here. Therefore, if the maximum actuation stretch is determined by LT, we should note that further actuation may be possible.

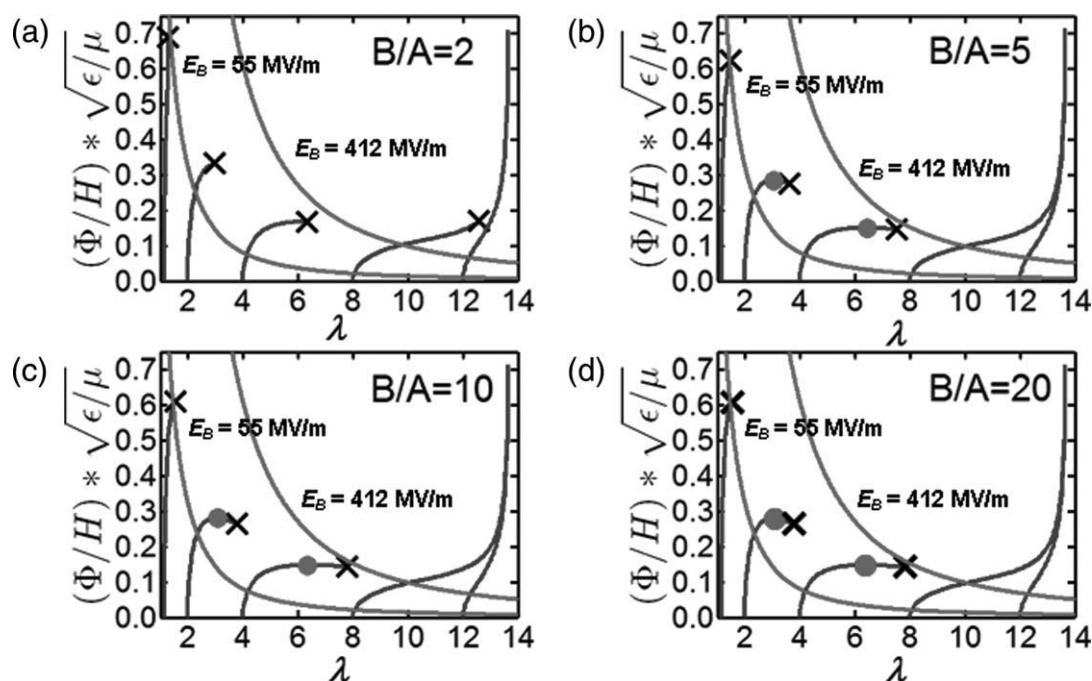


FIGURE 12 Actuation response of a circular actuator to an applied voltage at various levels of prestretch for: (a) $B/A = 2$; (b) $B/A = 5$; (c) $B/A = 10$; (d) $B/A = 20$. The solid dots (●) indicate the onset of electromechanical instability, the black cross (x) indicate loss of tension. The intersection between the red breakdown lines and the blue voltage-stretch response indicate electrical breakdown. The level of prestretch may be read from the blue lines at $\Phi = 0$. The two breakdown lines indicate experimentally measured dielectric strengths of 55 and 412 MV/m, at prestretches of 1.15 and 4.0, respectively.

Let us turn our focus on two specific values of prestretches: $\lambda_{pre} = 1.15$ and $\lambda_{pre} = 4.0$, corresponding to the experiment performed by Pelrine et al. in ref. 8. We compared our results with their experimental measurements in Table 1. Good agreement was found for both prestretches, validating our method.

CONCLUDING REMARKS

A DE actuation may respond to voltage in two ways: One that undergoes EMI, characterized by a peak in the voltage-stretch response (Type A), and the other with a monotonic voltage-stretch response (Type B). We found that EMI severely limits the maximum actuation strain. But when EMI is suppressed or eliminated, large actuation strains exceeding 100% may be attained. EMI may be suppressed or elimi-

nated by applying prestretch and/or selecting/designing another elastomer with a smaller limiting stretch. Phase diagrams can be generated for DEs of specific geometries under specific load configurations. The phase diagrams can be used as design tools to optimize the maximum actuation strain of a given DE. We used our method to analyze a circular DEA and found good agreement between our analysis and the experimental measurements. It is hoped that our theory will guide the design of DEAs that maximizes actuation performance.

ACKNOWLEDGMENTS

This work was partially funded by the Agency of Science, Technology and Research (A*STAR), Singapore, through the sponsoring of a two-year postdoctoral visit of S.J.A Koh to Harvard University, by the National Science Foundation (NSF) through a grant on Soft Active Materials, and by the Kavli Insitute at Harvard University. The work was also supported by the China Scholarship Council Foundation through the sponsoring of a one-year visit of T.F. Li to Harvard University. J.X. Zhou acknowledges the support of NSF (China) through 10872157 and 11072185. X.H. Zhao acknowledges the start-up funding from Pratt Engineering School, Duke University.

TABLE 1 Comparison of Maximum Actuation Stretch between Analysis and Experiment^a

B/A	Maximum Actuation Stretch (Linear)	
	Pre-stretch = 1.15	Pre-stretch = 4.00
2	1.12 ^a	1.58 ^a
5	1.27	1.59
10	1.27	1.59
20	1.28	1.59
Ref. [8]	1.18	1.61

^a Maximum actuation stretch determined by loss of tension.

REFERENCES AND NOTES

- Galler, N.; Ditzbacher, H.; Steinberger, B.; Hohenau, A.; Danschmuller, M.; Camacho-Gonzales, F.; Bauer, S.; Krenn, J. R.; Leitner, A.; Aussenegg, F. R. *Appl. Phys. B* **2006**, *85*, 7–10.

- 2 Kofod, G.; Paajanen, M.; Bauer, S. *Appl. Phys. A* **2006**, *85*, 141–143.
- 3 Kovacs, G.; During, L.; Michel, S.; Terrasi, G. *Sens. Actuators A* **2009**, *155*, 299–307.
- 4 Carpi, F.; Frediani, G.; Tarantino, S.; De Rossi, D. *Polym. Int.* **2010**, *59*, 407–414.
- 5 Keplinger, C.; Kaltenbrunner, M.; Arnold, N.; Bauer, S. *Proc. Natl. Acad. Sci.* **2010**, *107*, 4505–4510.
- 6 McKay, T.; O'Brien, B.; Calius, E.; Anderson, I. *Smart Mater. Struct.* **2010**, *19*, 055025.
- 7 Carpi, F.; DeRossi, D.; Kornbluh, R.; Pelrine, R.; Sommer-Larsen, P. *Dielectric Elastomers as Electromechanical Transducers*; Elsevier: Amsterdam, **2008**.
- 8 Pelrine, R.; Kornbluh, R.; Pei, Q.; Joseph, J. *Science* **2000**, *287*, 836–839.
- 9 Ha, S. M.; Yuan, W.; Pei, Q. B.; Pelrine, R. *Adv. Mater.* **2006**, *18*, 887–891.
- 10 Planté, J. S.; Dubowsky, S. *Int. J. Solids Struct.* **2006**, *43*, 7727–7751.
- 11 Moscardo, M.; Zhao, X.; Suo, Z.; Lapusta, Y. *J. Appl. Phys.* **2008**, *104*, 093503.
- 12 Koh, S. J. A.; Zhao, X.; Suo, Z. *Appl. Phys. Lett.* **2009**, *94*, 262902.
- 13 He, T.; Zhao, X.; Suo, Z. *J. Appl. Phys.* **2009**, *106*, 083522.
- 14 Zhenyi, M.; Scheinbeim, J. I.; Lee, J. W.; Newman, B. A. *J. Polym. Sci. Part B: Polym. Phys.* **1994**, *32*, 2721–2731.
- 15 Pelrine, R. E.; Kornbluh, R. D.; Joseph, J. P. *Sens. Actuators A* **1998**, *64*, 77–85.
- 16 Patrick, L.; Gabor, K.; Silvain, M. *Sens. Actuators A* **2007**, *135*, 748–757.
- 17 Keplinger, C.; Kaltenbrunner, M.; Arnold, N.; Bauer, S. *Appl. Phys. Lett.* **2008**, *92*, 192903.
- 18 Suo, Z.; Zhu, J. *Appl. Phys. Lett.* **2009**, *95*, 232909.
- 19 Zhao, X.; Suo, Z. *Phys. Rev. Lett.* **2010**, *104*, 178302.
- 20 Bochobza-Degani, O.; Elata, D.; Nemirovsky, Y. *Appl. Phys. Lett.* **2003**, *82*, 302–304.
- 21 Keplinger, C.; Kaltenbrunner, M.; Arnold, N.; Bauer, S. *Proc. Natl. Acad. Sci. USA* **2010**, *107*, 4505–4510.
- 22 Shankar, R.; Ghosh, T. K.; Spontak, R. J. *Adv. Mater.* **2007**, *19*, 2218–2223.
- 23 Kofod, G. *Dielectric Elastomer Actuators*, Ph.D. Thesis, The Technological University of Denmark, September **2001**.
- 24 Brochu, P.; Pei, Q. *Macromol. Rapid Commun.* **2010**, *31*, 10–36.
- 25 Kofod, G. *J. Phys. D* **2008**, *41*, 215405.
- 26 Stark, K. H.; Garton, C. G. *Nature* **1955**, *176*, 1225–1226.
- 27 Suo, Z. *Acta Mechanica Solida Sinica* **2010**, *23*, 549–578.
- 28 Zhao, X.; Hong, W.; Suo, Z. *Phys. Rev. B* **2007**, *76*, 134113.
- 29 Zhao, X.; Suo, Z. *Appl. Phys. Lett.* **2007**, *91*, 061921.
- 30 Vogan, J. D. *Development of Dielectric Elastomer Actuators for MRI Devices*, M.Sc. Thesis, Massachusetts Institute of Technology, Cambridge, MA, June **2004**.
- 31 Koh, S. J. A.; Keplinger, C.; Li, T.; Bauer, S.; Suo, Z. *IEEE/ASME Trans. Mech.* **2011**, *16*, 33–41.
- 32 Park, S. E.; Shrout, T. R. *J. Appl. Phys.* **1997**, *82*, 1804–1811.
- 33 Treloar, L. R. G. *Physics of Rubber Elasticity*, 3rd ed.; Clarendon Press: Oxford, **1975**; Chapter 5, pp 81–100.
- 34 Goulbourne, N.; Mockenstrum, E.; Frecker, M. *J. Appl. Mech.* **2005**, *72*, 899–906.
- 35 Wissler, M.; Mazza, E. *Smart Mater. Struct.* **2005**, *14*, 1396–1402.
- 36 Suo, Z.; Zhao, X.; Greene, W. H. *J. Mech. Phys. Solids* **2008**, *56*, 467–486.
- 37 Kofod, G.; Sommer-Larsen, P.; Kornbluh, R.; Pelrine, R. *J. Intell. Mater. Syst. Struct.* **2003**, *14*, 787–793.
- 38 Kuhn, W.; Grün, F. *Kolloidzshr* **1942**, *101*, 248–271.
- 39 Arruda, E. M.; Boyce, M. *J. Mech. Phys. Solids* **1992**, *41*, 389–412.
- 40 Ogden, R. W. *Proc. Roy. Soc. Lond. A* **1972**, *326*, 565–584.
- 41 Edwards, S. F.; Vilgis, T. *Polymer* **1985**, *27*, 483–492.
- 42 Carpi, F.; Migliore, A.; Serra, G.; De Rossi, D. *Smart Mater. Struct.* **2005**, *14*, 1–7.
- 43 Wissler, M.; Mazza, E. *Sens. Actuators A* **2007**, *134*, 494–504.
- 44 Zhao, X.; Suo, Z. *J. Appl. Phys.* **2008**, *104*, 123530.